AD-A051 567 MICHIGAN STATE UNIV EAST LANSING DEPT OF ELECTRICAL --ETC F/G 6/18
FOCAL HYPERTHERMIA AS INDUCED BY RF RADIATION OF SIMULACRA WITH--ETC(U)
1977 K CHEN, B S GURU DAAG29-76-G-0201

UNCLASSIFIED ARO-13448.11-L NL

| OF |
AD
A051567

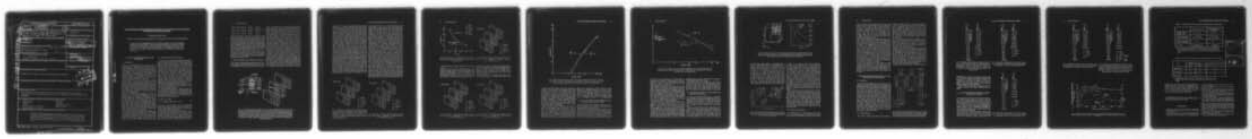

END
DATE
FILMED
4-78
DDC

(Data Entered)

REPORT DOCUMENTATION PAGE

READ INSTRUCTIONS BEFORE COMPLETING FORM

REPORT NUMBER (19) 13448.11-L (18) ARO	2. GOVT ACCESSION NO.
3. RECIPIENT'S CATALOG NUMBER	
4. TITLE (and Subtitle) (6) FOCAL HYPERTHERMIA AS INDUCED BY RF RADIATION OF SIMULACRA WITH EMBEDDED TUMORES AND AS INDUCED BY EM FIELDS IN A MODEL OF A HUMAN BODY,	5. TYPE OF REPORT & PERIOD COVERED: Reprint
	6. PERFORMING ORG. REPORT NUMBER
7. AUTHOR(s) (16) Kun-Mu Chen, B. S. Guru	8. CONTRACT OR GRANT NUMBER(s) (15) DAAG29-76-G-0201, NSF-ENG74-12603
9. PERFORMING ORGANIZATION NAME AND ADDRESS: Michigan State University, East Lansing, Michigan 48824 S/C 404255 D. of E. E. SS	10. PROGRAM ELEMENT, PROJECT, TASK AREA & WORK UNIT NUMBERS
11. CONTROLLING OFFICE NAME AND ADDRESS: U. S. Army Research Office, P. O. Box 12211, Research Triangle Park, NC 27709	12. REPORT DATE: (11) 1977
	13. NUMBER OF PAGES: 11 (12) 12p.
14. MONITORING AGENCY NAME & ADDRESS (if different from Controlling Office)	15. SECURITY CLASS. (of this report)
	15a. DECLASSIFICATION/DOWNGRADING SCHEDULE

16. DISTRIBUTION STATEMENT (of this Report)

Approved for public release; distribution unlimited.

17. DISTRIBUTION STATEMENT (of the abstract entered in Block 20, if different from Report)

18. SUPPLEMENTARY NOTES

The findings in this report are not to be construed as an official Department of the Army position, unless so designated by other authorized documents.

19. KEY WORDS (Continue on reverse side if necessary and identify by block number)

Hyperthermia
Simulacra
Tumors
Radiofrequency radiation
Electromagnetic fields
Biology
Heating
Energy absorption
Human models

20. ABSTRACT (Continue on reverse side if necessary and identify by block number)

In the first of two studies distributions of rates of EM energy absorption were observed in simulated biological bodies with embedded tumors. Part- and whole-body simulacra as irradiated by EM fields that ranged in frequency from 15 to 500 MHz exhibited differentially greater heating of tumors. Reduction of tumor conductivity resulted in enhancement of tumor heating. In the second study, a model of man was observed for induction of EM fields by 1 to 500-MHz energy. Greater rates of energy absorption occurred in regions of smaller cross sections and in tissues with lower conductivities.

DD FORM 1 JAN 73 1473 EDITION OF 1 NOV 65 IS OBSOLETE

Unclassified JOB

SECURITY CLASSIFICATION OF THIS PAGE (When Data Entered)

404 255

Focal hyperthermia as induced by RF radiation of simulacra with embedded tumors and as induced by EM fields in a model of a human body

Kun-Mu Chen and B. S. Guru

Department of Electrical Engineering and Systems Science, Michigan State University, East Lansing, Michigan 48824

In the first of two studies, distributions of rates of EM energy absorption were observed in simulated biological bodies with embedded tumors. Part- and whole-body simulacra as irradiated by EM fields that ranged in frequency from 15 to 500 MHz exhibited differentially greater heating of tumors. Reduction of tumor conductivity resulted in enhancement of tumor heating. In the second study, a model of man was observed for induction of EM fields by 1 to 500-MHz energy. Greater rates of energy absorption occurred in regions of smaller cross sections and in tissues with lower conductivities.

1. FOCAL HYPERTHERMIA INDUCED BY RF RADIATIONS

1.1. *Introduction.*

One of the promising therapies for cancer is that of hyperthermia in combination with chemotherapy or ionizing radiations. When the temperature of a tumor is raised a few degrees above that of surrounding tissues, accompanying chemo- or radio-therapy has been found to be effective in treating the tumor [*Overgaard,* 1976; *Suit and Shwayder,* 1974; *Robinson et al.,* 1974]. In the combined therapy of malignancies, the objective is to find a noninvasive method by which to heat the tumor without overheating other parts of the body.

In this paper, we report on attempts to discover effective means of inducing hyperthermia by HF and VHF EM fields in tumors that are embedded in simulated biological bodies. We found that effective local EM heating of the simulated tumor depends on (1) the type of irradiation, part or whole body; (2) the location of the tumor in the body; (3) the frequency of the EM field; and (4) the conductivity of the tumor relative to that of surrounding tissues.

First, we considered focal application of HF and VHF fields to a simulated biological body with an internal tumor. We studied the distribution of the specific absorption rate (SAR) of the EM energy in the body when the tumor conductivity was varied. We found that if the tumor were located in the central part of the body, a part-body irradiation with a uniform, HF or VHF electric field could induce a higher SAR in the tumor, resulting in selectively greater heating of the tumor. The local hyperthermia induced in the tumor could be enhanced if the tumor's conductivity was lower than that of surrounding tissues.

Next we investigated the scheme of local EM heating by increasing the local conductivity of the tumor, as suggested by *Ecker* [1975]. Our study indicates that increasing the conductivity of the tumor will not increase the absorption of energy by the tumor if the applied field is in the HF-VHF range of frequencies.

1.2. *Theoretical method and its accuracy.*

In this study, we considered a biological body of finite size with an embedded tumor. The body is partially or wholly radiated by EM energy in the HF-VHF range. Physically, the tumor is assumed to be a local region with a conductivity that differs from that of the surrounding tissue. The first step of our study was to determine the internal electric field inside the heterogeneous body as induced by the applied EM field. After this quantity was obtained, the SAR was determined. For convenience in reduction and reporting of SAR data, we have normalized rate of energy absorption (W) to volume (the cubic meter) instead of mass (the kilogram). Since the cubic centimeter of biological materials closely approximates one gram of mass, our SAR-datum can be interpreted as the watt per megagram (W/Mg), or the milliwatt per kilogram (mW/kg).

The theoretical method used in this study is based on a tensor integral equation [*Livesay and Chen,* 1974]. The method is briefly outlined.

If a finite biological body of arbitrary shape, with permittivity $\epsilon(\mathbf{r})$, conductivity of $\sigma(\mathbf{r})$ and permeability μ_0, is irradiated in free space by an electromagnetic wave with an electric field $\mathbf{E}^i(\mathbf{r})$, the total induced electric field $\mathbf{E}(\mathbf{r})$ inside the body can be determined from the following tensor integral equation:

$$[1 + \tau(\mathbf{r})/3j\omega\epsilon_0]\mathbf{E}(\mathbf{r}) - PV\int_v \tau(\mathbf{r}')\mathbf{E}(\mathbf{r}')\cdot\mathbf{G}(\mathbf{r},\mathbf{r}')dV' = \mathbf{E}^i(\mathbf{r}) \quad (1)$$

where $\tau(\mathbf{r}) = \sigma(\mathbf{r}) + j\omega(\epsilon(\mathbf{r}) - \epsilon_0)$, ϵ_0 is the free-space permittivity, the PV symbol means the principal value of the integral, $\mathbf{G}(\mathbf{r},\mathbf{r}')$ is the free space, tensor Green's function, and V is the body's volume.

If the body is partitioned into N subvolumes or cells, and $\mathbf{E}(\mathbf{r})$ and $\tau(\mathbf{r})$ are assumed to be constant within each cell, equation (1) can be transformed into $3N$ simultaneous equations for E_x, E_y, and E_z at the centers of N cells by the point-matching method. These simultaneous equations can be written into matrix form as

$$\begin{bmatrix} [G_{xx}] & [G_{xy}] & [G_{xz}] \\ [G_{yx}] & [G_{yy}] & [G_{yz}] \\ [G_{zx}] & [G_{zy}] & [G_{zz}] \end{bmatrix} \begin{bmatrix} [E_x] \\ [E_y] \\ [E_z] \end{bmatrix} = - \begin{bmatrix} [E_x{}^i] \\ [E_y{}^i] \\ [E_z{}^i] \end{bmatrix} \quad (2)$$

The $[G]$ matrix is a $3N$ by $3N$ matrix, while $[E]$ and $[E^i]$ are $3N$ column matrices that express the total electric field and the incident electric field at the centers of N cells. The elements of the $[G]$ matrix have been evaluated by *Livesay and Chen* [1974]. Therefore, with a known incident electric field $\mathbf{E}^i(\mathbf{r})$, the total induced electric field $\mathbf{E}(\mathbf{r})$ inside the body can be obtained from equation (2) by inverting the $[G]$ matrix. The induced current density is then determined from $\mathbf{J} = \tau \mathbf{E}$, and the rate of energy absorption from $P = 1/2\ \sigma |\mathbf{E}|^2$.

The accuracy of this method has been verified theoretically by a convergence test as described by *Livesay and Chen* [1974] and experimentally by an experiment conducted on a scaled model that contains a solution of saline [*Guru and Chen*, 1976].

1.3. *Part-body irradiation of a simulacrum with a tumor.*

We consider a biological body with dimensions of 6 by 6 by 12 cm and with an internal tumor of 2 by 2 by 4 cm embedded in the center of the body as shown in Figure 1. To this body, a uniform electric field ($\mathbf{E}^i$) of 1 V/m (maximum value) in the HF-VHF range is applied, from top to bottom and over the area of tumor, with a pair of plane electrodes. For the numerical calculation, one-half of the body is divided into 27 two-cm cubic cells, which are numbered as shown in Figure 1. The other half of the body is symmetrical to the first half. In this division of cells, the tumor occupies the 13th cell and the image of the 13th cell in the other half of the body. The uniform electric field $\mathbf{E}^i$ in the x direction is applied throughout the 10th, the 13th and the 16th cell and to their images in the other half of the body. Thus, $\mathbf{E}^i$ is applied across the top and bottom of the body over an area of 4 by 2 cm exclusively and $\mathbf{E}^i$ is zero over the rest of the body. Our aim was to determine the distribution of SARs in this simulated body with a tumor for several frequencies of radiation.

The first case to be considered is for the frequency of 15 MHz. At this frequency, the conductivity of the body is assumed to be 0.62 S/m and the dielectric constant, 150. The conductivity of the tumor is arbitrarily assumed to be one half of that of the surrounding tissue (0.31 S/m) and its dielectric constant is assumed to be the same as that of the surrounding tissue (150). While this assumption of a lower tumor conductivity is arbitrary, one may conjecture this condition as being due to a sluggish blood supply to the tumor, or this con-

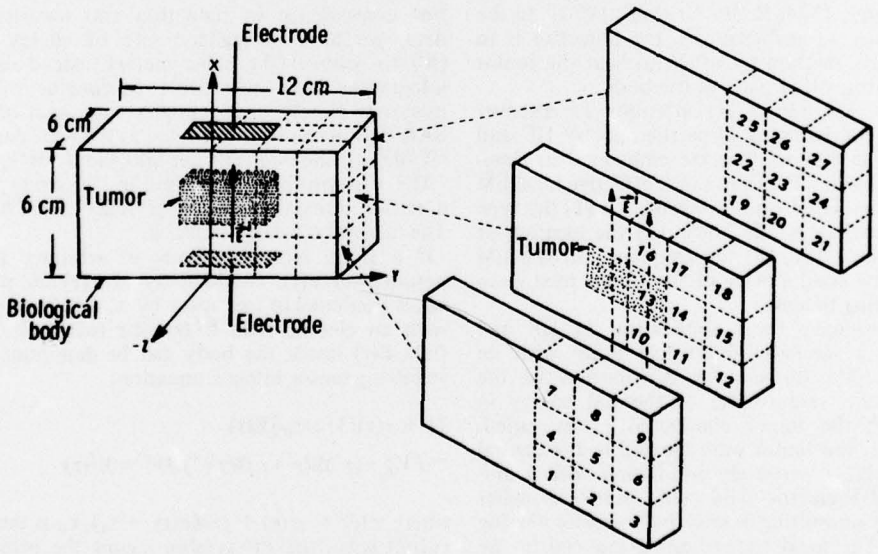

Fig. 1. A simulated biological body (6 by 6 by 12 cm) with an embedded tumor (2 by 2 by 4 cm) irradiated by a uniform electric field ($\mathbf{E}^i$) of 1 V/m (maximum value) at frequency (f) across the top and bottom of the body and over the area of the tumor. The uniform electric field is maintained by two parallel-plate electrodes. One half of the body is divided into 27 two-cm cubic cells. The tumor occupies the 13th cell and its image in the other half of the body. The uniform electric field $\mathbf{E}^i$ in the x direction is applied throughout the 10th, the 13th and the 16th cell and to their images in the other half of the body.

dition may be achieved surgically by blocking arterial circulation to the tumor after perfusing it with a fluid of low conductivity. It is noted at this point that we have also considered the cases of the tumor conductivity being the same or higher than that of the surrounding tissue. The findings of these cases are discussed later.

The distribution of SARs for this particular case is determined by the method described in the preceding section and the results are given in Figure 2. It is observed from Figure 2 that at the tumor, the SAR reaches a maximum value of 150.9 μW/m^3 (1 W/m^3 = mW/kg if the specific density is equal to 1), while the immediately neighboring cells, the 10th and the 16th cell, have an SAR of 44.8 μW/m^3. Over other parts of the body, only a small SAR is observed. This is expected since other parts of the body are not irradiated by the applied electric field. The interesting observation is that even though the immediately neighboring cells, the 10th and the 16th cell, are also irradiated, the SARs of these cells are only 0.3 times that of the tumor cell. This means that while the tumor is being heated intensively, the immediately neighboring tissue is only heated slightly. The physical explanation of this phenomenon is as follows: based on Maxwell's equation, $\nabla \cdot [(\sigma + j\omega\epsilon)\vec{E}] = 0$, the total induced current in the x direction is continuous through the 10th, the 13th and the 16th cell. Since the resistivity of the 13th cell is twice that of the 10th and the 16th cells, the SAR of the 13th cell should be higher than that of the 10th and the 16th cell by a factor of 2 as based on simple estimation. However, the body is of finite size and a careful theoretical quantification will predict the factor to be about 3.37 instead of 2. It is noted that this factor is not only a function of the conductivities of the tumor cell and of the neighboring cells but also depends strongly on the frequency of the applied electric field and on the body's geometry.

Next, we consider the case when the tumor's conductivity is 0.8 times that of the surrounding tissue, (0.496 S/m), while all other parameters are the same as those shown in Figure 2. Under this condition, the distribution of SARs in the simulated body with the tumor is shown in Figure 3. In comparing Figure 3 with Figure 2, one observes that the increase in the tumor's conductivity causes a decrease in the tumor's SAR from 150.9 μW/m^3 to 103.7 μW/m^3, while SARs in the surrounding tissues are only changed slightly. It is noted, however, that the SAR in the tumor is still more than twice that in the immediately neighboring tissues.

We have also considered the cases of the tumor's conductivity being the same, 1.2 times, or twice that of the surrounding tissue. The tumor's conductivities for these cases are 0.62 S/m, 0.744 S/m and 1.24 S/m, and the results for these cases are summarized in Figure 4. One observes that as the tumor's conductivity is increased, the SAR in the tumor tends to decrease while that in the immediately neighboring tissue remains relatively unchanged. The important point is that even if the tumor's conductivity is considerably higher than that of the surrounding tissue, the SAR in the tumor is still higher than that in the immediately neighboring tissue. This phenomenon is mainly due to the tumor's location in the central part of the body where the current induced by the electrodes reaches a maximum value in a standing wave pattern. It is understandable that if the tumor is located near the body's surface, the result will be different. A study of a more general case, which deals with a tumor in an arbitrary location within

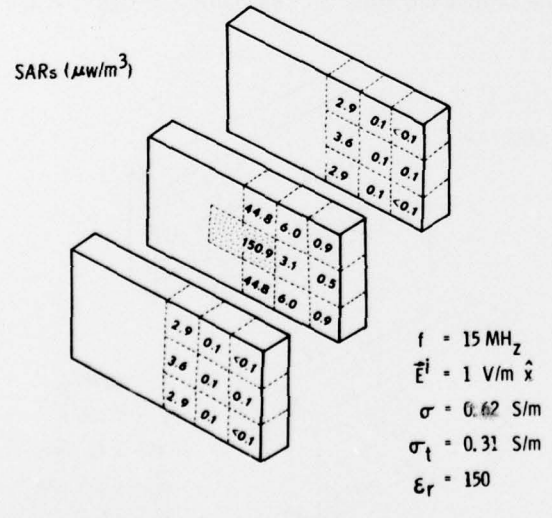

Fig. 2. Distribution of SARs inside the simulated biological body of Fig. 1 when the frequency (f) of the applied electric field ($\mathbf{E}^i$) is 15 MHz, the amplitude of $\mathbf{E}^i$ is 1 V/m, the conductivity of the body (σ) is 0.62 S/m, the conductivity of the tumor (σ_t) is 0.31 S/m, and the dielectric constant of the body and the tumor (ϵ_r) is 150.

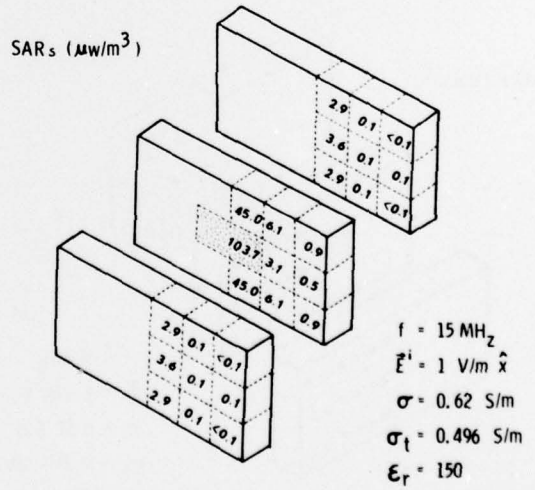

Fig. 3. Distribution of SARs inside the simulated biological body of Fig. 1 when $f = 15$ MHz, $\mathbf{E}^i = 1$ V/m $\hat{\mathbf{x}}$, $\sigma = 0.62$ S/m, $\sigma_t = 0.496$ S/m, and $\epsilon_r = 150$.

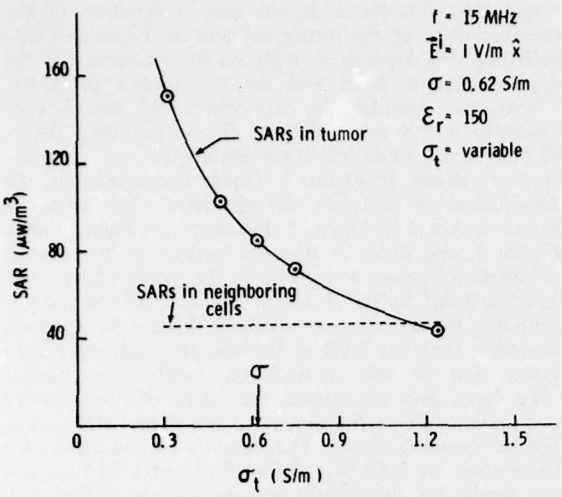

Fig. 4. SAR in the tumor as a function of the tumor's conductivity (σ_t) for the case of $f = 15$ MHz, $\mathbf{E}^i = 1$ V/m $\hat{\mathbf{x}}$, $\sigma = 0.62$ S/m, and $\epsilon_r = 150$.

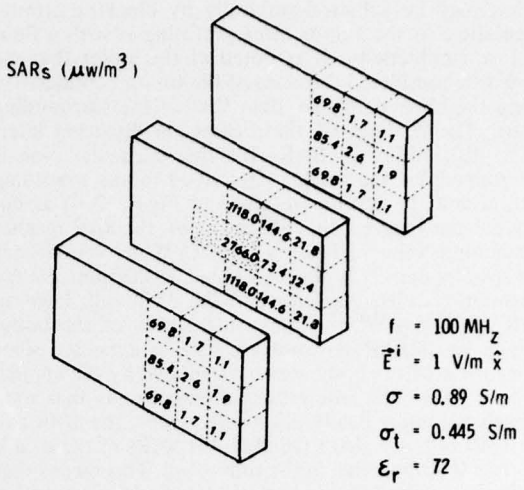

Fig. 6. Distribution of SARs inside the simulated biological body of Fig. 1 when $f = 100$ MHz, $\mathbf{E}^i = 1$ V/m $\hat{\mathbf{x}}$, $\sigma = 0.89$ S/m, $\sigma_t = 0.445$ S/m, and $\epsilon_r = 72$.

a simulated body, is being conducted at the present time.

Figures 5, 6 and 7 give the SAR distributions in the same heterogeneous body that is partially radiated by a uniform electric field of 1 V/m at 30 MHz, at 100 MHz, and at 500 MHz. In each of these examples, the conductivity of the tumor cell is assumed to be one-half of that of the body and the same permittivity is assumed for the tumor cell and for the body. In these figures, it is observed that the maximum SAR invariably occurs at the tumor and the value of the SAR tends to increase with the frequency of the applied electric field. The heating of neighboring tissues is also greater at higher frequencies.

Some other results on the SARs in the tumor and in the surrounding tissue are summarized in Figures 8 and

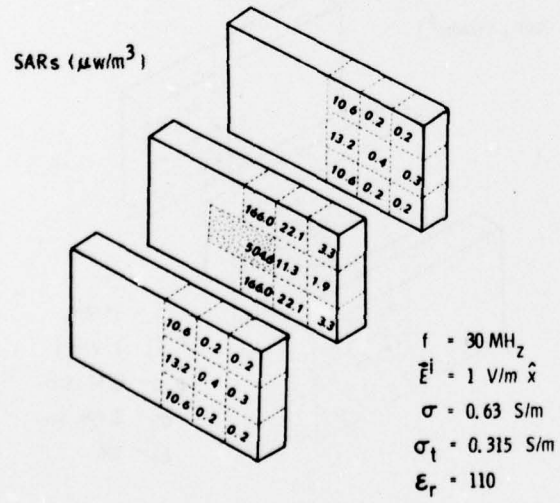

Fig. 5. Distribution of SARs inside the simulated biological body of Fig. 1 when $f = 30$ MHz, $\mathbf{E}^i = 1$ V/m $\hat{\mathbf{x}}$, $\sigma = 0.63$ S/m, $\sigma_t = 0.315$ S/m, and $\epsilon_r = 110$.

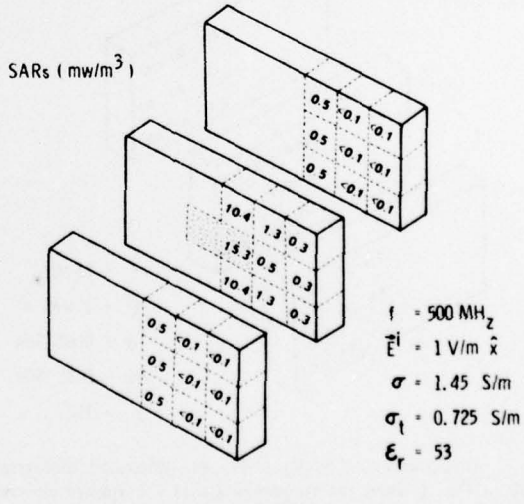

Fig. 7. Distribution of SARs inside the simulated biological body of Fig. 1 when $f = 500$ MHz, $\mathbf{E}^i = 1$ V/m $\hat{\mathbf{x}}$, $\sigma = 1.45$ S/m, $\sigma_t = 0.725$ S/m, and $\epsilon_r = 53$.

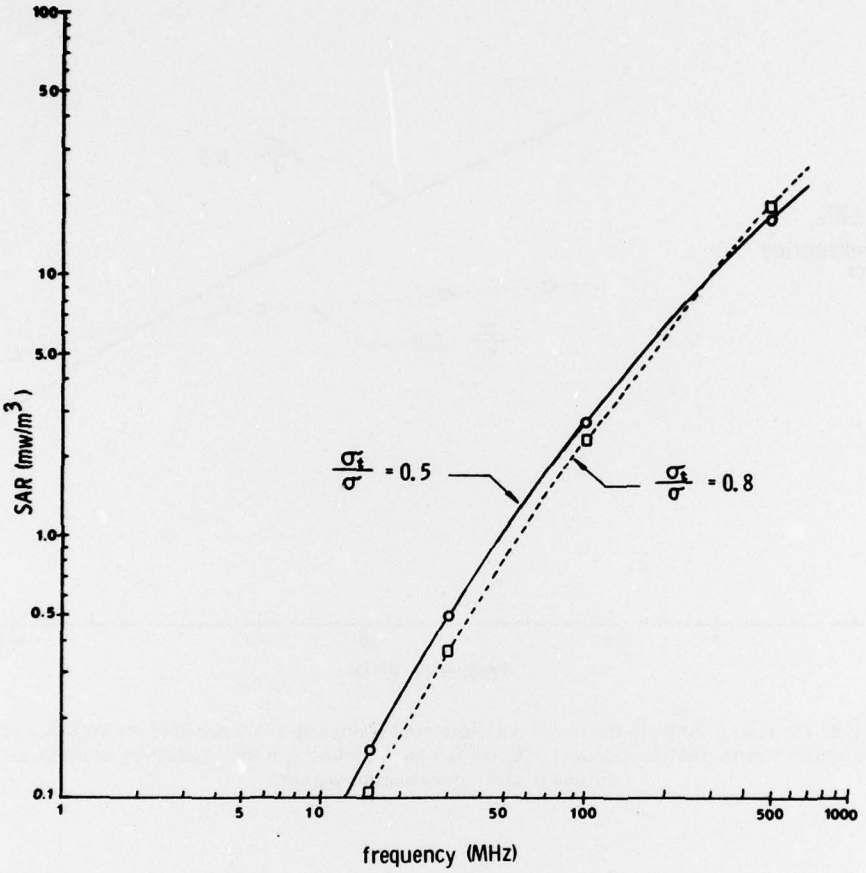

Fig. 8. Specific absorption rate in the tumor cell induced by an applied electric field of 1 V/m (maximum value) as a function of the frequency of the applied electric field for the cases of $\sigma_t/\sigma = 0.5$ and 0.8 where σ_t is the conductivity of the tumor cell and σ is that of the surrounding tissue.

9. Figure 8 shows the SAR of the tumor varying as a function of the frequency of the applied electric field for the cases of $\sigma_t/\sigma = 0.5$ and of 0.8, where σ_t is the conductivity of the tumor and σ is that of the body. It is observed in Figure 8 that the SAR at the tumor increases more steeply than linearly with increasing frequency of the applied electric field. This implies that at higher frequencies, it is easier to couple EM energy into tumors. However, from the engineering point of view, it is more difficult to generate a uniform electric field at higher frequencies with simple devices such as electrodes or parallel plates.

Figure 9 shows the ratio of SARs at the tumor cell and at the neighboring cells as a function of the frequency of the applied electric field for the cases of $\sigma_t/\sigma = 0.5$ and 0.8. For the case of $\sigma_t/\sigma = 0.5$, the ratio can be higher than 3 at 15 MHz and gradually decreases to 1.5 at 500 MHz. This means that at lower frequencies, the tumor can be heated intensively without severely heating the surrounding tissue. This advantage at lower frequencies is offset because it is more difficult to couple EM energy into the tumor at lower frequencies as indicated in Figure 8. For the case of $\sigma_t/\sigma = 0.8$, the ratio stays around 2 for the frequency range of 15 to 500 MHz. Thus, for this case, it may be more efficient from the viewpoint of energy coupling to use a 100-MHz field than a 15- or 30-MHz field.

1.4. *A body with embedded region of differing conductivity wholly irradiated by an EM field.*

We investigated the feasibility of heating a tumor within a biological body via whole-body irradiation as suggested recently by *Ecker* [1975].

We consider a biological body with dimensions of 24 by 24 by 18 cm having a local region of variable conductivity with dimensions of 12 by 12 by 6 cm embedded in the center of the body as shown in Figure 10. A vertically polarized EM wave of 30 MHz with an electric field of 1 V/m (maximum value) is incident normal to

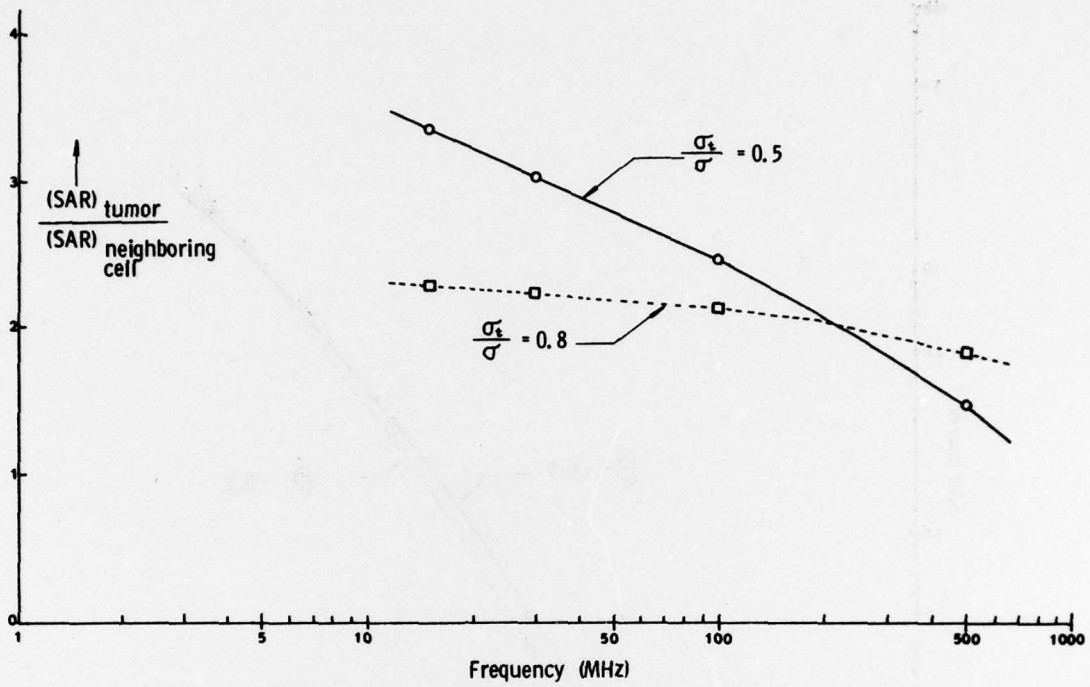

Fig. 9. The ratio of SARs in the tumor cell and in neighboring cells as a function of the frequency of the applied electric field for the cases of $\sigma_t/\sigma = 0.5$ and 0.8 where σ_t is the conductivity of the tumor cell and σ is that of the neighboring cells.

the body. The conductivity of the local region is changed from 0.6 S/m to 100 S/m while that at any other point of the body is kept constant at 0.6 S/m. A dielectric constant of 100 is assumed for the local region and for the rest of the body.

We attempted to determine the changes in the induced electric field, in the induced current density and in the SAR in the local region when its conductivity is varied. In the numerical calculation of the induced field, the body is subdivided into 48 cells with each cell being a 6-cm cube. Owing to the symmetry in the x-y plane, only one-fourth of the volume of body is shown divided into cells. The induced electric field at the center of each cell is determined first and then the induced current density and the SAR are calculated.

In Figure 10, the x component (the dominant component) of the induced electric field, E_x, the x component of the induced current density, J_x, and the SAR, $P = \sigma/2\ (E_x^2 + E_y^2 + E_z^2)$, at the center of the cell belonging to the local region are shown as functions of the conductivity of the local region. It is observed in Figure 10 that as the conductivity of the local region is increased, the induced current density, J_x, increases initially and then stays constant while both the induced electric field, E_x, and the SAR, P, decrease. Although not shown in Figure 10, the value of E_x, J_x and P at neighboring cells are nearly unaffected by the change of the conductivity in the local region.

From these results, it is evident that the attempt selectively to heat a tumor in a biological body by using an electric field of HF range and increasing the conductivity of the tumor is not effective. At higher frequencies and with other body geometries, the results may be different, as discussed in the next section.

1.5. *Experimental verification with scaled models irradiated by microwave energy.*

To verify our theoretical predictions, an experiment was conducted on saline-solution models that were irradiated by a microwave field at 2370 MHz. The reason for conducting the experiment at a microwave frequency rather than at one in the HF range was due to the size of the available anechoic chamber and other limitations.

Figure 11 shows theoretical and experimental results on the EM heating of a local region with variable conductivity in a rectangular plastic box containing a saline solution. The box, with dimensions of 8 by 6 by 2 cm, was partitioned into three regions with the surrounding regions (region 2) containing saline of a fixed concentration ($\sigma_2 = 2.2$ S/m, $\epsilon_2 = 76.22\ \epsilon_0$)

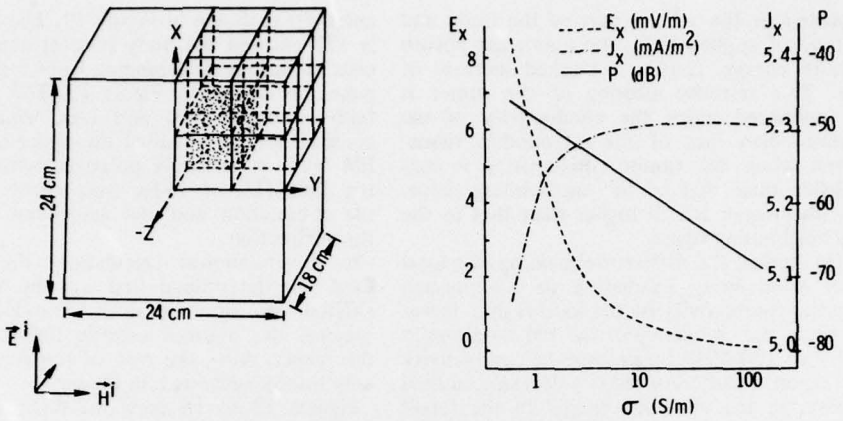

Fig. 10. Theoretical results on the x components of the induced electrical field and induced current density and the SAR at the center of the cell belonging to the central block as functions of the conductivity of the block, induced by a vertically polarized EM wave of 30 MHz at normal incidence. The conductivity of the rest of the biological body is kept at 0.6 S/m.

and the central region (region 1) containing saline of varying concentrations. This box was irradiated by a vertically polarized EM wave of 2370 MHz at normal incidence. The induced electric field in the vertical direction, E_x, was measured at a point (x = 0.5 cm, y = 0.5 cm, z = 1.5 cm) in region 1 as the saline concentration of the region was increased. The increase of concentration results in a linear increase of the conductivity and some change in the permittivity of region 1. The rate of energy absorption due to the vertical component of the induced electric field, $1/2\ \sigma E_x^2$, was then determined. The experimental results were compared with the corresponding theoretical results and excellent agreement was obtained.

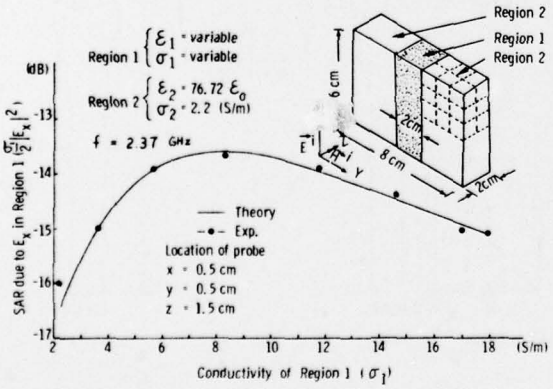

Fig. 11. Theoretical and experimental results on the SARs in region 1 as a function of the conductivity in the same region of a saltwater model, induced by a vertically polarized EM wave of 2.37 GHz at normal incidence.

In Figure 11 it is observed that as the conductivity of region 1 is increased, the rate of energy absorption increases initially but then decreases as the conductivity is increased beyond 8.5 S/m. This indicates that at 2370 MHz there exists an optimal conductivity for the local region to gain the most effective EM heating.

The findings in this section are somewhat different from those discussed in preceding sections. The difference is probably due the heterogeneous body of Figure 11, which is quite different from those of previous cases in which radiation at a much lower frequency was applied. Furthermore, the incident electric field is parallel to the boundary of the central region; thus, the induced currents in the central region and the surrounding regions can be discontinuous. Given these departures, the physical phenomena involved and the physical explanation provided in Section 3 cannot be applied.

One is reminded that the main purpose of the experimental study is to verify the validity and accuracy of a method that is based on the tensor integral equation when applied to a heterogeneous body. The excellent agreement between theory and experiment as shown in Figure 11 serves the intended purpose. The empirical results of this section also indicate that the rate of energy absorption in a local region within a biological body depends strongly on the body's geometry, the electrical properties of the local region and other parts of the body, and the frequency and polarization of the applied EM field.

1.6. *Conclusion and discussion.*

An embedded tumor of conductivity that differs from that of surrounding tissue was irradiated by a focalized electric field in the HF-VHF range. We found that if the

tumor is located in the central part of the body and under this type of applied field, the tumor can absorb relatively more energy, causing a marked increase of temperature. This selective heating of the tumor is particularly enhanced when the conductivity of the tumor is lower than that of the surrounding tissue; however, even when the tumor conductivity is considerably higher than that of the surrounding tissue, the SAR in the tumor is still higher than that in the immediately neighboring tissue.

We have also studied the differential heating of a local region under whole-body irradiation in combination with varying the conductivity of the local region. It was found that when the frequency of the EM field was in the range of 1 to 100 MHz, an increase of conductivity of the local region usually resulted in a decrease, instead of an increase, in the absorbed energy in the target region. For a microwave field, there might exist an optimal conductivity for the local region to gain the most effective EM heating. However, microwave heating would not be effective if the tumor were deep inside the body because of lessened depth of penetration.

It is important to note that while an electric field of HF-VHF range may not be effective in heating a tumor with a higher conductivity, a magnetic field of HF range may be used to heat this type of tumor.

In the actual application of EM heating, one may encounter overheating of fat or bone, which have lower conductivities than that of surrounding muscle. The overheating may be avoided if the applied field can be focused at the tumor. In addition, potential burns of the skin can be avoided by cooling of the body's surface by air.

2. INTERNAL EM FIELDS INDUCED BY VHF AND UHF WAVES IN A HUMAN BODY

2.1. *Introduction.*

In the study of biological effects of EM waves and in medical applications of EM radiation, it is important and desirable to quantify the internal fields and SARs that are induced in the human body by EM radiation. We report here some numerical results on a model of the human body as radiated by EM waves of 1 to 500 MHz and of both vertical and horizontal polarization. The effect due to the electrical heterogeneity of the body is considered and the phenomenon of resonance is also discussed. The results in this paper are considered to be more accurate than those we reported in a previous paper [*Chen and Guru,* 1976], which was based on a simpler, homogeneous body. A method based on a tensor integral equation [*Livesay and Chen,* 1974] as described in a previous section has been used in the numerical calculations. Many other results not reported in this paper are available in another report [*Chen and Guru,* 1977]. Some theoretical results are compared with existing experimental results.

2.2. *Numerical results.*

The model of human body used in the numerical calculations is shown in Figure 12. The height of the body is 177 cm and the body is constructed with 108 cubic cells of various sizes ranging from 5-cm cubes to 12-cm cubes, as shown in Figure 12. The front layer of the body includes arms and legs, while the back layer consists only of a half of the upper torso. The incident EM wave is vertically polarized with an incident electric field ($\mathbf{E}^i$) of 1V/m (maximum value) directed in the x direction and the associated magnetic field in the y direction.

In the numerical calculation, the induced electric field was determined first and the SAR was then calculated from the relation of $1/2\,\sigma|\mathbf{E}|^2$. For the sake of brevity, the induced electric field is not reported in this paper. Also, the case of horizontal polarization is only briefly addressed, in Figure 18.

Figures 13 to 16 show the distributions of SARs in the human body that is schematized in Figure 12 when the incident EM wave is at frequencies of 30, 80, 200, and 500 MHz. By examining Figures 13 and 14, it is observed that for the lower part of the VHF band, the incuced EM field inside a typical adult body is mainly concentrated in the regions of the legs and the neck. For the upper part of VHF band and beyond, the regions of higher SARs can be in the arms, the neck or other parts of the torso. In general, higher SARs occur in the regions with smaller cross-sectional areas.

Figure 17 shows the distribution of SARs induced by a

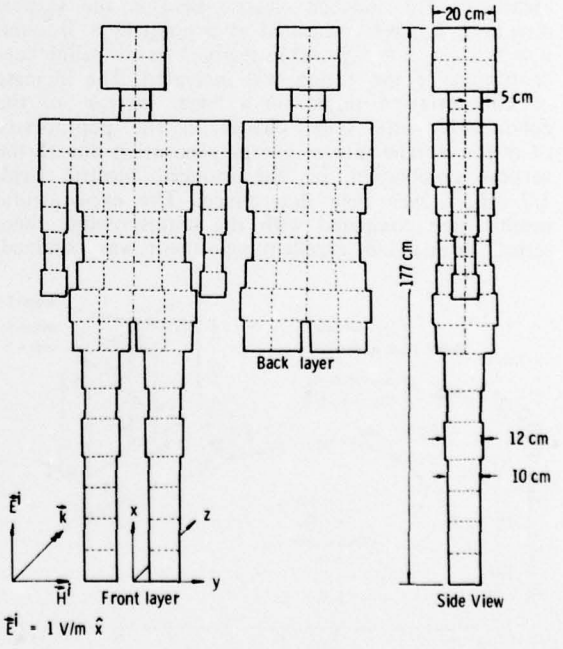

Fig. 12. Geometry of a simulated human body of 1.77 m high used in the theoretical field quantification. The body is divided into 108 cubic cells of various sizes. A vertically polarized, plane EM wave of frequency (f) with an incident electric field of 1 V/m (maximum value) is incident normally upon the body.

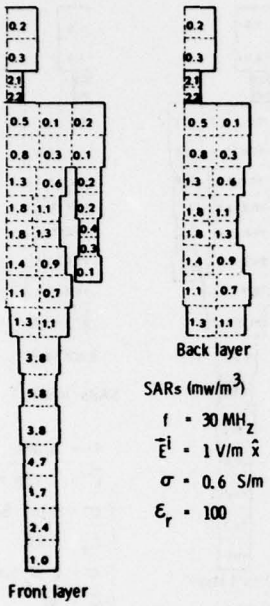

Fig. 13. Distribution of SARs inside the human-body model of Fig. 12 when the incident EM wave is vertically polarized, the frequency (f) is 30 MHz, the amplitude of the incident electric field ($\mathbf{E}^i$) is 1 V/m (maximum value), the conductivity of the body (σ) is 0.6 S/m, and the dielectric constant of the body (ϵ_r) is 100.

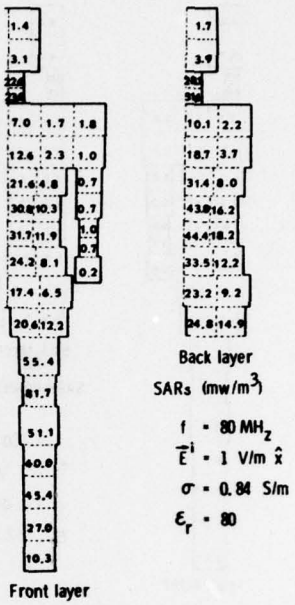

Fig. 14. Distribution of SARs inside the human-body model of Fig. 12 when the incident EM wave is vertically polarized, $f = 80$ MHz, $\mathbf{E}^i = 1$ V/m $\hat{\mathbf{x}}$, $\sigma = 0.84$ S/m, and $\epsilon_r = 80$.

80-MHz EM wave inside a heterogeneous human body. In this example, a region of low conductivity with 0.045 S/m (and $\epsilon_r = 9.83$) such as lungs, is assumed to be embedded in a body with a conductivity of 0.84 S/m (and $\epsilon_r = 80$). The results indicate a greatly enhanced SAR in the region of low conductivity.

Figure 18 shows both the rate of energy absorption as expressed in terms of the relative absorption area, A_r, where

$$A_r = \frac{\text{rate of energy absorption/incident power density,}}{\text{total surface area of body}}$$

and the maximum induced electric field (normalized by the incident electric field), as functions of the frequency of the incident EM waves for both vertical and horizontal polarizations and for the frequency range of 1 to 500 MHz. For the case of vertical polarization, a major resonance is clearly observed at about 80 MHz and weaker resonances occur at 160 MHz and 240 MHz. For the horizontal polarization, only a single weak resonant peak is observed near 200 MHz.

Some theoretical results are compared in Table 1 with experimental results of *Gandhi* [1975] and in Table 2 with experimental results of *Guy et al.* [1976]. Qualitatively, the theoretical results compare well with

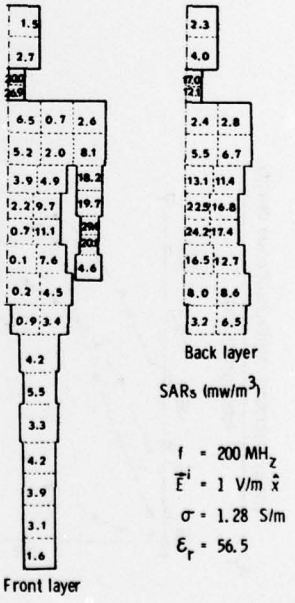

Fig. 15. Distribution of SARs inside the human-body model of Fig. 12 when the incident EM wave is vertically polarized, $f = 200$ MHz, $\mathbf{E}^i = 1$ V/m $\hat{\mathbf{x}}$, $\sigma = 1.28$ S/m, and $\epsilon_r = 56.5$.

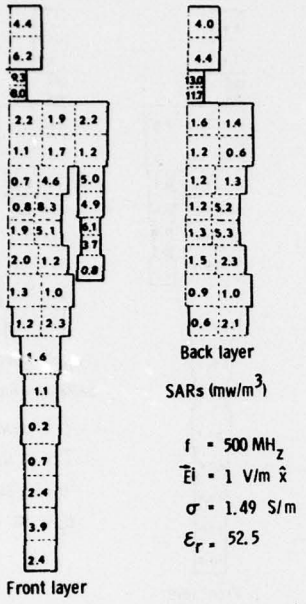

Fig. 16. Distribution of SARs inside the human-body model of Fig. 12 when the incident EM wave is vertically polarized, $f = 500$ MHz, $\mathbf{E}^i = 1$ V/m $\hat{\mathbf{x}}$, $\sigma = 1.49$ S/m, and $\epsilon_r = 52.5$.

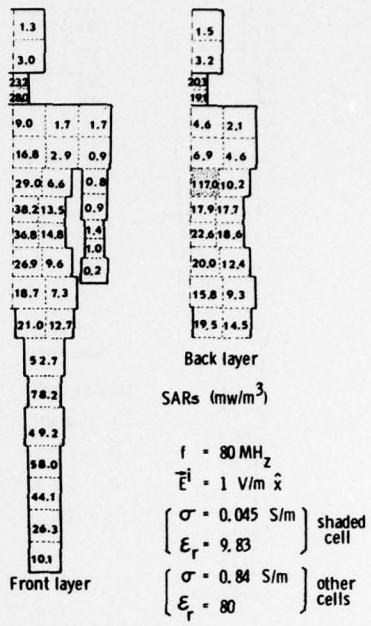

Fig. 17. Distribution of SARs inside the human-body model of Fig. 12 with a heterogeneous region of low conductivity and permittivity as indicated by a shaded area in the back layer. For the heterogeneous region, $\sigma = 0.045$ S/m, $\epsilon_r = 9.83$; for the rest of the body, $\sigma = 0.84$ S/m, $\epsilon_r = 80$. The incident EM wave is vertically polarized, $f = 80$ MHz, and $\mathbf{E}^i = 1$ V/m $\hat{\mathbf{x}}$.

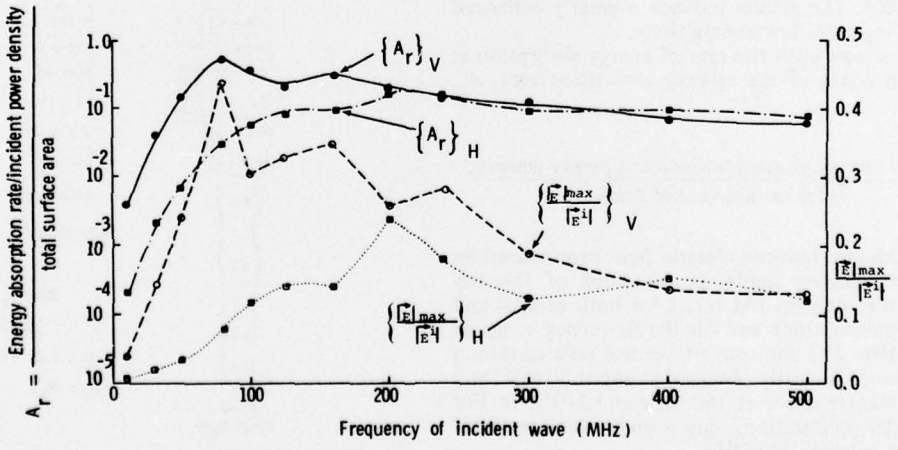

Fig. 18. Relative absorption area and relative maximum induced electric field in the body of a 1.77 m adult as functions of the frequency of vertically polarized and horizontally polarized incident EM waves.

TABLE 1. Comparison of theoretical results with experimental results of *Gandhi* [1975].

	Theoretical results	Experimental Results by Gandhi
Resonant height of body (L)	$L/\lambda_o = 0.472$	$L/\lambda_o = 0.4$
Pesonant frequency for an adult body	f = 80 MHz (for L = 1.77 m)	f = 65∿75 MHz (for L = 1.75 m)
Effective absorption area at resonance*	3.2	3∿4
Hot spots	hot spots in legs and neck area	hot spot at neck area

*The effective absorption area was defined as [(energy absorption rate/incident power density) / physical-shadow area] by Gandhi. It is different from the relative absorption area defined in this paper.

TABLE 2. Comparison of theoretical results with experimental results of *Guy et al.* [1976]

SAR	Theoretical results		Exp. results by Guy et al.** (figs. 8 and 11 of ref. 6)
	30 MHz	80 MHz	
legs (mW/m^3)	12.6	163	54
neck (mW/m^3)	4.5	60	27
arms (mW/m^3)	low	low	low

**Experimental results were for 31 MHz EM waves with an incident electric field of 1 V/m (rms value) and for a body of 1.74 m height.

Gandhi's data. Our results on the general distribution of SARs compare very well with the experimental results of *Guy et al.* which are based on a 31-MHz field. However, the absolute values of SARs deviate by a factor of 4 to 5 between theory and experiment. The source of deviation is not known at the present time.

Acknowledgments. This research was supported by U. S. Army Research Office under Grant DAAG 29-76-G-0201 and in part by NSF under Grant ENG 74-12603.

REFERENCES

Chen, Kun-Mu, and B. S. Guru (1976), Induced EM field and absorbed power density inside a human torso, *Proc. IEEE, 64*(9), 1450-1453.

Chen, Kun-Mu, and B. S. Guru (1977), Internal EM field and absorbed power density induced by 1 to 500 MHz EM waves inside human torsos with realistic models, a technical report, Division of Engineering Research, Michigan State University, E. Lansing, Michigan.

Ecker, H. A. (1975), Biomedical applications of EM radiation, *Microwave J.*, 47-50.

Gandhi, O. P. (1975), Condition of strongest electromagnetic power deposition in man and animals, *IEEE Trans. Microwave Theory Tech., MTT-23*(12), 1021-1029.

Guru, B. S., and Kun-Mu Chen, (1976), Experimental and theoretical studies on electromagnetic fields induced inside finite biological bodies, *IEEE Trans. Microwave Theory Tech., MTT-24*,(7), 433-440.

Guy, A. W., M. D. Webb, and C. C. Sorenson (1976), Determination of power absorption in man exposed to high frequency electromagnetic field by thermographic measurements in scale models, *IEEE Trans. Biomed. Eng., BME-23*(5), 361-371.

Livesay, D., and Kun-Mu Chen (1974), Electromagnetic field induced inside arbitrarily shaped biological bodies. *IEEE Trans. Microwave Theory Tech., MTT-22*(12), 1273-1280.

Overgaard, J. (1976), Combined adriamycin and hyperthermia treatment of a murine mammary carcinoma *in vivo, Cancer Res., 36*, 3077-3081.

Robinson, J. E., M. J. Wizenberg, and W. A. McCready (1974), Radiation and hyperthermal response of normal tissue *in situ, Radiology, 113*(1), 195-198.

Suit, H. D., and M. Shwayder (1974), Hyperthermia: potential as an antitumor agent, *Cancer, 34*(1), 122-129.